Redox–Chemical Core Manipulation of $[Os_{18}Hg_3C_2(CO)_{42}]^{2-}$; Synthesis and Crystal Structure of the Cluster $[Os_{18}Hg_2C_2(CO)_{42}]^{4-}$†

Lutz H. Gade,[a] Brian F. G. Johnson,[a] Jack Lewis,*[,a] Gráinne Conole[b] and Mary McPartlin*[,b]

[a] *University Chemical Laboratory, Lensfield Road, Cambridge CB2 1EW, UK*

[b] *School of Chemistry, The University of North London, Holloway Road, London N7 8DB, UK*

The extrusion of metallic mercury from $[Os_{18}Hg_3C_2(CO)_{42}]^{2-}$ **1** by reduction has been studied and the tetraanionic cluster $[Os_{18}Hg_2C_2(CO)_{42}]^{4-}$ **3** isolated and characterised. The structure of the $[N(PPh_3)_2]^+$ salt of **3** has been established by a single-crystal X-ray structure analysis. Oxidation of **3** with $[Fe(\eta^5\text{-}C_5H_5)_2]BF_4$ yielded the corresponding tri- and di-anionic clusters **4** and **2**. The clusters **1**–**4** were found to be interrelated by reversible photochemical and redox–chemical transformations. This reactive behaviour is reflected in the results of an electrochemical study of **1** by cyclic voltammetry.

The systematic build-up and selective manipulation of high-nuclearity cluster cores remains one of the greatest synthetic challenges in inorganic chemistry.[1] The condensation of cluster fragments with heterometal electrophiles provides not only a comparatively straightforward and rational approach to cluster aggregation but also generates specific interfaces within the metal core where subsequent structural modifications may occur.

We have recently studied the chemical reactivity of the octadecaosmiumtrimercury cluster dianion $[Os_{18}Hg_3C_2(CO)_{42}]^{2-}$ **1** which contains a triangular Hg_3 subunit sandwiched between two tricapped-octahedral $Os_9C(CO)_{21}$ fragments.[2] This mixed-metal cluster, with clear-cut borderlines between its metallic domains, has proved to be an ideal substrate for site-specific modifications of the metal core. The concept of local labilisation of the cluster framework through the introduction of metal–metal bond polarity in **1** has found its most prominent manifestation in the photolytic extrusion of a mercury atom, generating the dimercury dianion $[Os_{18}Hg_2C_2(CO)_{42}]^{2-}$ **2**. This process has been found to be reversible, with a complete reinsertion of the extruded metal taking place on removal of the source of radiation (Scheme 1).[3,4]

The photochemical extrusion of a mercury atom from compound **1** to generate **2** was interpreted as being a consequence of a metal–metal charge-transfer transition to an Os–Hg or Hg–Hg antibonding cluster valence orbital.[4] This effectively amounts to a photochemically driven redox reaction which leads to the local destabilisation of the cluster core. It was therefore of interest to investigate whether the removal of a mercury atom from the cluster could also be achieved by redox–chemical (in this case reductive) means.

Results and Discussion

Synthesis and Structure of $[N(PPh_3)_2]_4[Os_{18}Hg_2C_2(CO)_{42}]$.—Titration of a solution of $[Os_{18}Hg_3C_2(CO)_{42}]^{2-}$ **1** with a solution of $[Co(\eta^5\text{-}C_5H_5)_2]$ in tetrahydrofuran (thf) leads to the generation of a new Os–Hg cluster **3** and the conversion is complete after the addition of 2 molar equivalents of cobaltocene. The symmetry of the infrared ν(CO) absorption band pattern of **3** is almost identical to that of the starting material, albeit shifted to lower wavenumbers by 25–28 cm^{-1} (Table 1). For an osmium cluster of nuclearity *ca.* 20 this corresponds to an increase in negative charge by two units. This along with the stoichiometry of the redox titration led to the proposal of a tetraanionic Os–Hg cluster as the reaction product. The similarity of the infrared ν(CO) band pattern and the ^{13}CO NMR signal pattern to those of the trimercury **1** and the dimercury **2** dianions was indicative of a $[Os_9C(CO)_{21}]_xHg_y$ core similar to that of these known clusters.[2,4] Since the molecular ion peak in the negative-ion fast atom bombardment (FAB) mass spectrum was consistent with an octadecaosmiumdimercury cluster, the product of **3** was formulated as $[Os_{18}Hg_2C_2(CO)_{42}]^{4-}$. Thus **3** is a partially demercuriated compound similar to the photolysis product **2**, but with an increased negative charge as a consequence of the direct reduction used, as opposed to the intramolecular redox process in the photolytic conversion of **1** into **2** which leaves the charge of the species unchanged.

Structurally characterised examples of high-nuclearity clusters in different oxidation states remain rare, in spite of the invaluable information about the relationship between the

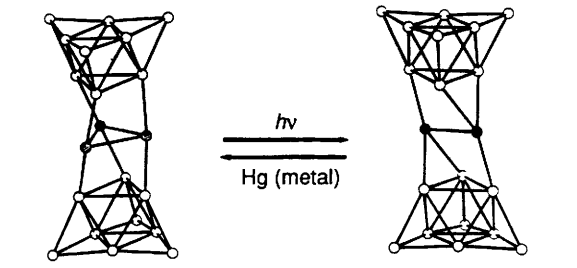

$[Os_{18}Hg_3C_2(CO)_{42}]^{2-}$ **1** $[Os_{18}Hg_2C_2(CO)_{42}]^{2-}$ **2**

Scheme 1

Table 1 Infrared data (cm^{-1}) for the mixed-metal clusters **1**–**4**

Compound	ν(CO)	Ref.
1 $[Os_{18}Hg_3C_2(CO)_{42}]^{2-}$	2072m, 2057s, 2005s[a]	2*a*, 4
2 $[Os_{18}Hg_2C_2(CO)_{42}]^{2-}$	2064s, 2057vs, 2006s[a]	3
3 $[Os_{18}Hg_2C_2(CO)_{42}]^{4-}$	2047m, 2029s, 1980s[b]	This work
4 $[Os_{18}Hg_2C_2(CO)_{42}]^{3-}$	2051s, 2044vs, 1994s[a]	This work

[a] In CH_2Cl_2. [b] In acetone.

† *Supplementary data available:* see Instructions for Authors, *J. Chem. Soc., Dalton Trans.*, 1992, Issue 1, pp. xx–xxv.

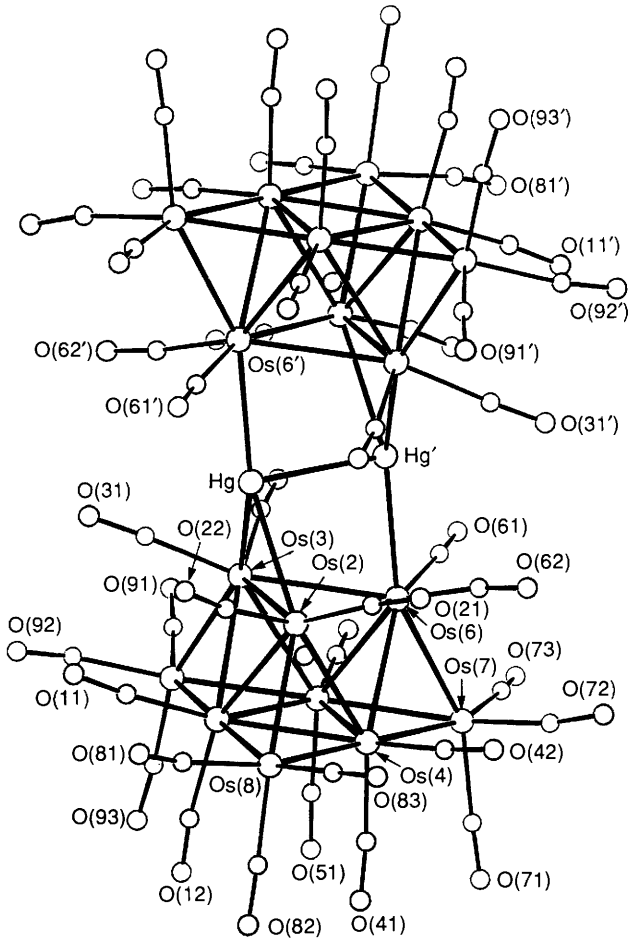

Fig. 1 The structure of the tetraanion $[Os_{18}Hg_2C_2(CO)_{42}]^{4-}$ **3** showing the numbering scheme; the C and O atoms of each carbonyl ligand have the same number and the first digit is that of the relevant Os atom

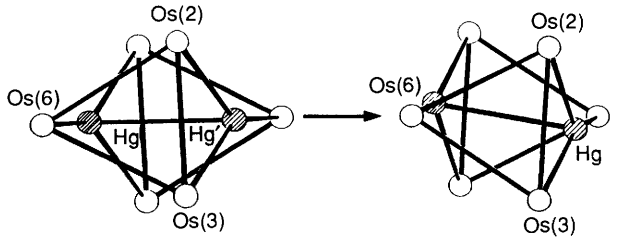

Fig. 2 Structural changes accompanying the transformation of compound **2** into **3** viewed along an axis perpendicular to the Os_3 triangles Os(2)–Os(3)–Os(6)

electronic and molecular structure of a cluster that can be derived from X-ray diffraction studies of such species. One such example for which two oxidation states has been structurally characterised is $[Rh_{12}C_2(CO)_{24}]^{x-}$ (x = 2 or 3).[5]

In view of the known structure of compound **2**, the effect on the metal-core geometry of the addition of two electronic charges and the relationship of this new structure to that of the starting material **1** was of considerable interest. The latter was particularly important in order to assess whether the synthetic strategy of a selective and local core modification by redox–chemical means found its justification in the reaction product **3**. Single-crystal structure analysis of the $[N(PPh_3)_2]^+$ salt of **3** established the structure of the cluster tetraanion shown in Fig. 1; the principal bond lengths and angles are listed in Table 2 and the atomic coordinates in Table 3. The overall structure closely resembles that of the dianion **2**, the major change being a 'straightening up' of the 'slipped sandwich' arrangement of the two Os_9 clusters found in **2**; the line joining

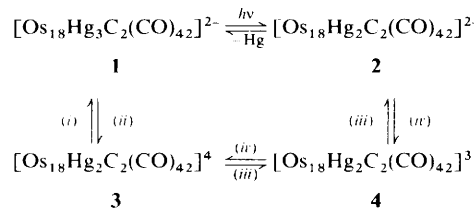

Scheme 2 The network of reversible photo- and redox-chemical transformations linking compounds **1**–**4**. (*i*) $[Co(\eta^5\text{-}C_5H_5)_2]$; (*ii*) Hg^{2+}; (*iii*) $[Fe(\eta^5\text{-}C_5H_5)_2]^+$; (*iv*) $[Co(\eta^5\text{-}C_5H_5)_2]$ or Na–Ph_2CO

the centroids of the two symmetry-related triangles defined by Os(2), Os(3) and Os(6) is at a nearly orthogonal angle of 83.54° to these uncapped faces, whereas in **2** a more oblique angle of 77.97° was observed. The straightening up of the metal framework may be a consequence of the removal of the 'electron deficiency' in **2** by the presence of the two extra electrons. The structural change is best appreciated on viewing each molecule in a direction perpendicular to the triangle Os(2),Os(3),Os(6) (Fig. 2). In the 'slipped' configuration of **2** a closer packing of the two parallel Os_3 triangles and the dimercury fragment occurs than in the structure of **3**. The contraction in the framework on going from **1** to **2** is removed when the latter straightens up to give **3** with a resultant increase in the perpendicular distance between the two Os_9 cluster units by 0.32 Å. Additionally, the Hg–Hg distance has increased significantly from 2.744(5) Å in **2** to 2.820(3) Å in **3**.

The principal structural changes that accompany the transformations linking compounds **1**–**3** appear to be restricted to the decapped triangular Os_3 faces of the $Os_9C(CO)_{21}$ units and the linking Hg_x fragment (x = 2 or 3), the osmium domains of the cluster being barely affected. This peculiarity of the structural transformation is reflected in the ^{13}C NMR spectra of the clusters (Fig. 3). The ^{13}CO resonance which is most significantly shifted on going from **1** to **2**, and further to **3**, is that of the carbonyl ligands co-ordinated to the two equivalent Os_3 triangles adjacent to the Hg_x unit in each structure which has a set of $^2J(^{199}Hg\text{–}^{13}C)$ satellites associated with it. The photolytic extrusion of Hg on going from **1** to **2** effects a downfield shift of this signal by 2 ppm from δ 177.7 to 179.7, while on reduction to the tetraanion **3** it is further shifted to δ 187.1, a change which is much more drastic than that of the other CO resonances of the cluster. In addition to their effect on the shift of this set of ^{13}CO nuclei, the core transformations in these clusters have a particularly pronounced effect on the chemical shift of the interstitial carbide which changes from δ 397.4 in **1** to δ 411.1 in **2** and back to δ 390.1 on reduction to **3**. Due to the lack of theoretical insight into the chemical shifts of interstitial atoms in cluster structures it is at this stage impossible to correlate these data with the different electronic structures of the $Os_9C(CO)_{21}$ fragments in the cluster obtained so far.[6]

The tetraanion in compound **3** is oxidised with $[Fe(\eta^5\text{-}C_5H_5)_2][BF_4]$ to the corresponding trianion $[Os_{18}Hg_2C_2(CO)_{42}]^{3-}$ **4** [IR: ν(CO) 2051s, 2044vs and 1994s cm^{-1}] and on reaction with a second equivalent of the oxidant to the dianion **2**. Conversely, **4** and **3** can be selectively generated by reduction of **2** with 1 and 2 equivalents of $[Co(\eta^5\text{-}C_5H_5)_2]$ respectively, thus establishing the total reversibility of these redox reactions. While reaction of the dianion **2** with the tetraanion **3** leads to redox comproportionation to yield the trianion **4**, the reaction of **3** with highly dissociated mercury(II) salts such as $Hg(O_3SCF_3)_2$ regenerates the dianionic trimercury cluster **1**. The reversible transformations which link **1** and **2**–**4** are summarised in Scheme 2.

Electrochemical Study of the Transformations linking Compounds **1**–**4**.—The routine application of electrochemical techniques in the study of the redox properties of transition-metal clusters is a relatively recent development.[7] In particular,

Table 2 Selected bond lengths (Å) and interbond angles (°) for the tetraanion **3**

Os(1)–Os(2)	2.886(2)	Os(1)–Os(3)	2.888(2)	Os(4)–Os(6)	2.888(2)	Os(4)–Os(7)	2.776(2)
Os(1)–Os(4)	2.863(2)	Os(1)–Os(5)	2.869(2)	Os(4)–Os(8)	2.771(2)	Os(5)–Os(6)	2.871(2)
Os(1)–Os(8)	2.783(2)	Os(1)–Os(9)	2.788(2)	Os(5)–Os(7)	2.782(2)	Os(5)–Os(9)	2.772(2)
Os(2)–Os(3)	3.092(2)	Os(2)–Os(4)	2.894(2)	Os(6)–Os(7)	2.816(2)	Os(2)–Hg	2.813(2)
Os(2)–Os(6)	3.006(2)	Os(2)–Os(8)	2.761(2)	Os(3)–Hg	2.898(2)	Os(6)–Hg′	2.747(2)
Os(3)–Os(5)	2.929(2)	Os(3)–Os(6)	3.011(2)	Hg–Hg′	2.820(3)		
Os(3)–Os(9)	2.748(2)	Os(4)–Os(5)	2.830(2)				
Os(6)–Os(2)–Os(3)	59.2(1)	Os(3)–Os(2)–Hg	58.6(1)	C(32)–Os(3)–Os(9)	98(1)	C(32)–Os(3)–C(31)	92(2)
C(21)–Os(2)–Os(1)	151(1)	C(21)–Os(2)–Os(3)	140(1)	Os(3)–Os(6)–Os(2)	61.8(1)	Hg′–Os(6)–Os(2)	85.5(1)
C(21)–Os(2)–Os(4)	95(1)	C(21)–Os(2)–Os(6)	88(1)	Hg′–Os(6)–Os(3)	79.4(1)	Hg′–Os(6)–C(61)	79(1)
C(21)–Os(2)–Os(8)	98(1)	C(21)–Os(2)–Hg	99(1)	Hg′–Os(6)–C(62)	81(1)	C(61)–Os(6)–Os(2)	159(1)
C(22)–Os(2)–Os(1)	99(1)	C(22)–Os(2)–Os(3)	110(1)	C(61)–Os(6)–Os(3)	102(1)	C(61)–Os(6)–Os(4)	138(1)
C(22)–Os(2)–Os(4)	139(1)	C(22)–Os(2)–Os(6)	161(1)	C(61)–Os(6)–Os(5)	92(1)	C(61)–Os(6)–Os(7)	81(1)
C(22)–Os(2)–Os(8)	81(1)	C(22)–Os(2)–C(21)	94(2)	C(62)–Os(6)–Os(2)	96(1)	C(62)–Os(6)–Os(3)	151(1)
C(22)–Os(2)–Hg	76(1)	Os(6)–Os(3)–Os(2)	59.0(1)	C(62)–Os(6)–Os(4)	95(1)	C(62)–Os(6)–Os(5)	144(1)
Os(2)–Os(3)–Hg	55.9(1)	C(31)–Os(3)–Os(1)	100(1)	C(62)–Os(6)–Os(7)	87(1)	C(62)–Os(6)–C(61)	94(1)
C(31)–Os(3)–Os(2)	107(1)	C(31)–Os(3)–Os(5)	143(1)	Os(2)–Hg–Hg′	88.0(1)	Os(3)–Hg–Hg′	80.2(1)
C(31)–Os(3)–Os(6)	158(1)	C(31)–Os(3)–Os(9)	85(1)	Os(2)–Hg–Os(6′)	154.0(1)	Os(3)–Hg–Os(6′)	139.6(1)
C(31)–Os(3)–Hg	74(1)	C(32)–Os(3)–Hg	101(1)	Os(6′)–Hg–Hg′	90.3(1)		
C(32)–Os(3)–Os(1)	152(1)	C(32)–Os(3)–Os(2)	141(1)				
C(32)–Os(3)–Os(5)	97(1)	C(32)–Os(3)–Os(6)	91(1)				

Compound	δ(CO)	δ(carbide)	Ref.
1 $[Os_{18}Hg_3C_2(CO)_{42}]^{2-}$	185.7 (6 CO), 184.9 (6 CO), 177.7 [12 CO, $^2J(^{199}Hg-^{13}C)$ = 56 Hz], 175.6 (18 CO)	397.4	2*a*, 4
2 $[Os_{18}Hg_2C_2(CO)_{42}]^{2-}$	185.8 (6 CO), 185.7 (6 CO), 179.7 [12 CO, $^2J(^{199}Hg-^{13}C)$ not resolved], 176.0 (18 CO)	411.1	3
3 $[Os_{18}Hg_2C_2(CO)_{42}]^{4-}$	190.1 (6 CO), 187.1 [12 CO, $^2J(^{199}Hg-^{13}C)$ = 42 Hz], 186.3 (6 CO), 178.9 (18 CO)	390.1	This work

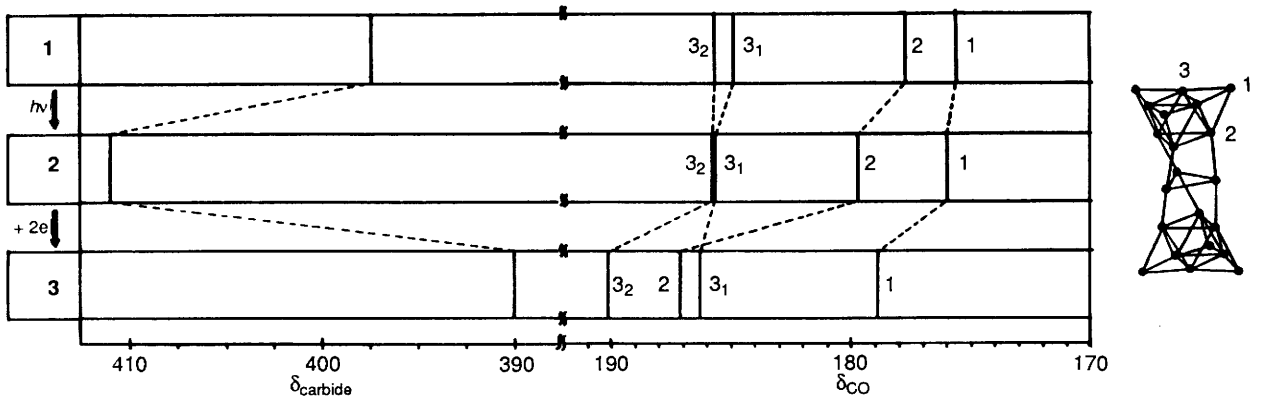

Fig. 3 Comparison of the ^{13}CO and [^{13}C]carbide chemical shifts found for compounds **1**–**3**

there are only a few examples of electrochemical investigations of high-nuclearity clusters to date.[8] In the light of the redox-chemical activity of compounds **1** and **2** discussed above it was desirable to quantify these observations by electrochemically probing the transformations generating **3** and **4**. Fig. 4 shows the cyclic voltammogram of a solution of **1** in CH_2Cl_2 for a scan range of +700 to −1000 mV *vs.* Ag–AgCl. The cycle between +700 and −500 mV (*a*) shows the absence of any redox activity of the cluster within this region. However, on scanning to −1000 mV at a scan rate of 100 mV s^{-1}, an irreversible reduction wave is observed with a cathodic peak current of −840 mV. Associated with this reduction wave are two anodic peaks at +160 and +330 mV (*b*). Their intensity increases markedly if the sample is electrolysed at −1000 mV for 10 s before the reverse scan, which makes them a 'spectral fingerprint' of the reduction product generated between −800 and −1000 mV. Its identity was established by a series of cyclic voltammograms recorded after successive irradiation of a solution of **1** with a 250 W tungsten lamp (Fig. 5).

Irradiation of compound **1**, in solution, leads to extrusion of Hg and generation of the dianionic dimercury cluster **2**. In the cyclic voltammogram (Fig. 5) this transformation is manifested in the appearance of two sets of cathodic and anionic waves with current peaks at +270, +100 mV and +330, +160 mV, respectively, while the intensity of the irreversible reduction wave below −800 mV gradually decreases. The latter may therefore be interpreted as representing a reduction of $[Os_{18}Hg_3C_2(CO)_{42}]^{2-}$ **1** with subsequent extrusion of an Hg atom to yield a species which is consequently formulated as $[Os_{18}Hg_2C_2(CO)_{42}]^{x-}$ ($x > 2$). This Hg extrusion step on reduction is expected to diminish in intensity on photolytic depletion of the solution of the trimercury cluster **1**, as is indeed observed in Fig. 5. The 'anodic fingerprint' in Fig. 4 is therefore assigned as the two-step reoxidation of $[Os_{18}Hg_2C_2(CO)_{42}]^{x-}$ to the dianion **2**. The reversibility of the two redox waves (i_a/i_c = 1; $i_p \approx v^{\frac{1}{2}}$) at $E_{\frac{1}{2}}$ = +300 and +130 mV and their identity as one-electron redox processes enables an interpretation of the cyclic voltammogram in Fig. 5: the irreversible reduction below −800 mV represents the overall process (1), generating the tetraanionic

$$[Os_{18}Hg_3C_2(CO)_{42}]^{2-} + 2e \longrightarrow \underset{\mathbf{1}}{} \quad [Os_{18}Hg_2C_2(CO)_{42}]^{4-} + Hg \quad (1)$$
$$\mathbf{3}$$

dimercury cluster **3** which is reoxidised in two one-electron steps at E_{ox} = +170 and +340 mV to yield the corresponding cluster dianion **2**. If the scan is performed on a solution of the

Table 3 Fractional atomic coordinates for compound **3**

Atom	*x*	*y*	*z*	Atom	*x*	*y*	*z*
Os(1)	0.301 35(8)	0.336 47(9)	0.065 64(10)	C(123)	0.087 4(15)	−0.084 0(14)	0.083 2(16)
Os(2)	0.458 92(8)	0.412 78(8)	0.132 25(9)	C(124)	0.118 9(15)	−0.004 3(14)	0.094 9(16)
Os(3)	0.340 02(9)	0.414 16(8)	−0.058 91(9)	C(125)	0.183 8(15)	0.020 3(14)	0.171 5(16)
Os(4)	0.433 06(8)	0.238 94(8)	0.123 37(9)	C(126)	0.217 1(15)	−0.034 8(14)	0.236 4(16)
Os(5)	0.324 75(9)	0.238 17(9)	−0.051 86(10)	C(131)	0.227 1(17)	−0.150 2(18)	0.400 5(17)
Os(6)	0.480 45(8)	0.314 07(8)	0.004 20(9)	C(132)	0.268 8(17)	−0.193 0(18)	0.474 3(17)
Os(7)	0.454 56(9)	0.145 65(9)	0.007 68(11)	C(133)	0.268 5(17)	−0.171 3(18)	0.550 1(17)
Os(8)	0.408 44(10)	0.330 98(10)	0.237 36(10)	C(134)	0.226 5(17)	−0.106 7(18)	0.552 1(17)
Os(9)	0.196 11(9)	0.331 08(9)	−0.107 56(11)	C(135)	0.184 9(17)	−0.063 9(18)	0.478 3(17)
Hg	0.457 49(9)	0.544 50(8)	0.030 25(10)	C(136)	0.185 2(17)	−0.085 7(18)	0.402 5(17)
C	0.390 3(16)	0.329 9(16)	0.034 8(18)	C(211)	0.438 4(13)	−0.081 3(11)	0.324 9(16)
C(11)	0.260 9(21)	0.432 3(19)	0.088 0(24)	C(212)	0.483 9(13)	−0.057 5(11)	0.284 3(16)
O(11)	0.238 4(15)	0.490 8(14)	0.095 6(17)	C(213)	0.523 6(13)	0.018 8(11)	0.301 0(16)
C(12)	0.228 1(19)	0.260 0(20)	0.085 5(22)	C(214)	0.517 8(13)	0.071 4(11)	0.358 5(16)
O(12)	0.190 9(16)	0.212 0(16)	0.090 7(18)	C(215)	0.472 4(13)	0.047 5(11)	0.399 1(16)
C(21)	0.568 0(22)	0.413 3(22)	0.202 5(24)	C(216)	0.432 6(13)	−0.028 8(11)	0.382 4(16)
O(21)	0.632 9(17)	0.407 6(17)	0.245 1(19)	C(221)	0.348 9(14)	−0.205 8(16)	0.194 3(13)
C(22)	0.447 0(23)	0.500 7(24)	0.189 0(26)	C(222)	0.319 4(14)	−0.147 7(16)	0.132 0(13)
O(22)	0.445 7(18)	0.561 4(19)	0.223 6(20)	C(223)	0.286 3(14)	−0.170 0(16)	0.046 1(13)
C(31)	0.283 0(23)	0.510 1(21)	−0.077 1(27)	C(224)	0.282 7(14)	−0.250 4(16)	0.022 5(13)
O(31)	0.249 2(16)	0.564 4(16)	−0.084 7(19)	C(225)	0.312 2(14)	−0.308 6(16)	0.084 8(13)
C(32)	0.336 4(25)	0.419 8(26)	−0.169 0(21)	C(226)	0.345 3(14)	−0.286 3(16)	0.170 7(13)
O(32)	0.332 1(20)	0.411 0(21)	−0.233 4(19)	C(231)	0.463 1(14)	−0.254 2(16)	0.363 9(18)
C(41)	0.382 2(20)	0.146 3(20)	0.146 9(22)	C(232)	0.526 6(14)	−0.261 9(16)	0.346 6(18)
O(41)	0.350 7(17)	0.097 2(17)	0.165 7(19)	C(233)	0.581 5(14)	−0.318 1(16)	0.389 9(18)
C(42)	0.530 8(14)	0.214 2(16)	0.200 6(17)	C(234)	0.573 0(14)	−0.366 6(16)	0.450 5(18)
O(42)	0.597 8(15)	0.205 2(18)	0.252 7(18)	C(235)	0.509 5(14)	−0.359 0(16)	0.467 8(18)
C(51)	0.262 6(24)	0.146 1(25)	−0.047 6(27)	C(236)	0.454 6(14)	−0.302 7(16)	0.424 5(18)
O(51)	0.228 7(16)	0.089 3(17)	−0.043 5(18)	C(311)	0.069 3(18)	−0.319 9(23)	0.730 8(20)
C(52)	0.302 7(21)	0.219 0(21)	−0.167 2(24)	C(312)	0.066 1(18)	−0.402 9(23)	0.718 1(20)
O(52)	0.289 8(18)	0.207 0(18)	−0.235 0(20)	C(313)	0.121 0(18)	−0.435 6(23)	0.698 2(20)
C(61)	0.481 3(25)	0.284 7(26)	−0.103 0(30)	C(314)	0.179 2(18)	−0.385 3(23)	0.691 1(20)
O(61)	0.474 9(19)	0.268 3(19)	−0.164 7(22)	C(315)	0.182 4(18)	−0.302 3(23)	0.703 8(20)
C(62)	0.587 5(22)	0.301 1(22)	0.071 3(24)	C(316)	0.127 4(18)	−0.269 6(23)	0.723 7(20)
O(62)	0.651 1(19)	0.289 7(19)	0.117 8(21)	C(321)	−0.004 4(17)	−0.326 5(15)	0.836 6(15)
C(71)	0.414 1(25)	0.045 4(26)	0.036 8(28)	C(322)	−0.073 1(17)	−0.334 4(15)	0.846 0(15)
O(71)	0.392 2(18)	−0.012 5(19)	0.051 2(20)	C(323)	−0.070 8(17)	−0.364 6(15)	0.921 0(15)
C(72)	0.558 7(27)	0.114 3(27)	0.074 0(30)	C(324)	0.000 3(17)	−0.387 0(15)	0.986 6(15)
O(72)	0.623 7(19)	0.103 1(18)	0.107 4(21)	C(325)	0.068 9(17)	−0.379 2(15)	0.977 2(15)
C(73)	0.446 9(23)	0.104 7(23)	−0.095 3(21)	C(326)	0.066 7(17)	−0.348 9(15)	0.902 2(15)
O(73)	0.429 9(17)	0.080 2(17)	−0.161 9(16)	C(331)	0.017 1(19)	−0.173 2(15)	0.776 3(20)
C(81)	0.369 6(30)	0.412 9(27)	0.283 7(33)	C(332)	0.087 3(19)	−0.154 2(15)	0.849 8(20)
O(81)	0.359 7(23)	0.464 0(21)	0.315 1(25)	C(333)	0.107 4(19)	−0.074 8(15)	0.880 7(20)
C(82)	0.358 4(26)	0.253 7(25)	0.278 8(31)	C(334)	0.057 3(19)	−0.014 5(15)	0.838 2(20)
O(82)	0.323 6(19)	0.206 1(18)	0.297 6(21)	C(335)	−0.013 0(19)	−0.033 6(15)	0.764 8(20)
C(83)	0.505 2(23)	0.324 5(22)	0.333 4(25)	C(336)	−0.033 1(19)	−0.112 9(15)	0.733 8(20)
O(83)	0.567 5(22)	0.315 8(22)	0.389 3(25)	C(411)	−0.202 6(12)	−0.219 1(12)	0.530 0(15)
C(91)	0.165 0(28)	0.331 6(28)	−0.222 3(34)	C(412)	−0.230 8(12)	−0.196 6(12)	0.445 4(15)
O(91)	0.148 0(24)	0.341 6(25)	−0.293 4(29)	C(413)	−0.289 3(12)	−0.142 1(12)	0.411 3(15)
C(92)	0.132 5(37)	0.416 7(33)	−0.111 8(43)	C(414)	−0.319 6(12)	−0.110 2(12)	0.461 8(15)
O(92)	0.100 2(17)	0.464 1(17)	−0.100 4(20)	C(415)	−0.291 5(12)	−0.132 8(12)	0.546 5(15)
C(93)	0.119 8(22)	0.247 0(22)	−0.120 8(29)	C(416)	−0.233 0(12)	−0.187 2(12)	0.580 6(15)
O(93)	0.074 5(19)	0.202 3(20)	−0.116 9(24)	C(421)	−0.188 8(14)	−0.391 0(14)	0.535 7(18)
P(1)	0.235 4(6)	−0.182 5(6)	0.312 5(7)	C(422)	−0.195 1(14)	−0.443 0(14)	0.595 3(18)
P(2)	0.388 8(5)	−0.181 7(6)	0.304 8(6)	C(423)	−0.238 7(14)	−0.517 0(14)	0.568 7(18)
N(1)	0.326 1(19)	−0.187 2(20)	0.340 6(22)	C(424)	−0.276 0(14)	−0.539 2(14)	0.482 6(18)
P(3)	−0.006 3(5)	−0.276 1(6)	0.747 8(6)	C(425)	−0.269 7(14)	−0.487 3(14)	0.423 0(18)
P(4)	−0.133 3(6)	−0.296 1(7)	0.570 1(6)	C(426)	−0.226 2(14)	−0.413 2(14)	0.449 6(18)
N(2)	−0.090 3(16)	−0.286 8(19)	0.668 1(19)	C(431)	−0.070 6(15)	−0.288 0(20)	0.522 3(19)
C(111)	0.181 1(14)	−0.279 1(12)	0.277 0(16)	C(432)	−0.041 8(15)	−0.210 7(20)	0.514 2(19)
C(112)	0.111 7(14)	−0.292 7(12)	0.284 5(16)	C(433)	0.018 0(15)	−0.200 7(20)	0.489 7(19)
C(113)	0.068 0(14)	−0.366 8(12)	0.258 7(16)	C(434)	0.049 0(15)	−0.268 0(20)	0.473 5(19)
C(114)	0.093 6(14)	−0.427 2(12)	0.225 5(16)	C(435)	0.020 2(15)	−0.345 3(20)	0.481 6(19)
C(115)	0.163 0(14)	−0.413 6(12)	0.218 0(16)	C(436)	−0.039 6(15)	−0.355 3(20)	0.506 1(19)
C(116)	0.206 8(14)	−0.339 5(12)	0.243 8(16)	C(1s)	−0.144 2(25)	−0.052 5(25)	0.297 6(28)
C(121)	0.185 6(15)	−0.114 5(14)	0.224 7(16)	Cl(s1)	−0.227 4(13)	0.008 3(17)	0.241 3(16)
C(122)	0.120 7(15)	−0.139 1(14)	0.148 1(16)	Cl(s2)	−0.080 3(14)	−0.007 7(16)	0.385 4(17)

dimercury dianion **2**, generated by extrusion of mercury on photolysis of **1**, the dianion is reversibly reduced *via* the trianion **4** to the tetraanion **3** (E_{red} = +270, +100 mV) but shows virtually no redox activity in the region between −800 and −1000 mV (*vs.* Ag–AgCl). The cyclovoltammetric study discussed here offers only a few clues as to the detailed mechanism of the formal two-electron reduction step and the concomitant ejection of the mercury atom from the cluster core. Since the

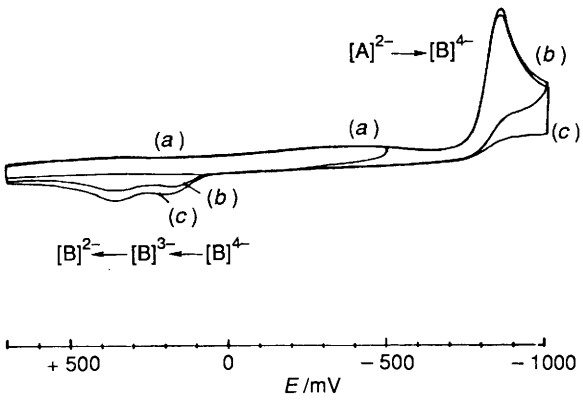

Fig. 4 Cyclic voltammogram of compound **1** recorded in CH_2Cl_2: potentials *vs.* Ag–AgCl; scan rate 100 mV s^{-1}. Scans: (*a*) from +700 to −500 mV, (*b*) from +700 to −1000 mV and (*c*) as (*b*) but with 10 s of electrolysis at −1000 mV. A = $Os_{18}Hg_3C_2(CO)_{42}$, B = $Os_{18}Hg_2C_2(CO)_{42}$

$$[N(PPh_3)_2]_2[Os_{18}Hg_3C_2(CO)_{42}] \xrightarrow{h\nu} [N(PPh_3)_2]_2[Os_{18}Hg_2C_2(CO)_{42}]$$

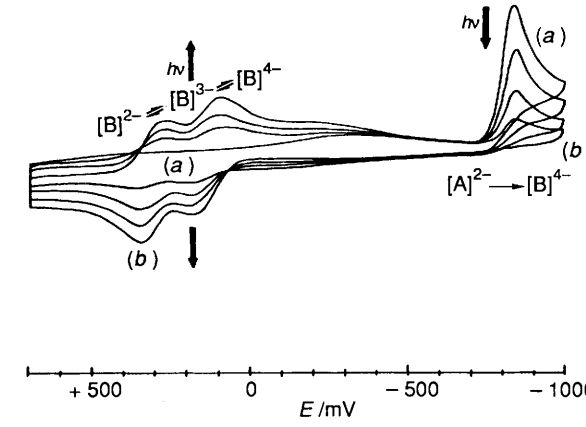

Fig. 5 Series of cyclic voltammograms recorded on successive irradiation of a solution of compound **1**, showing its conversion into **2**–**4**: (*a*) $[N(PPh_3)_2][A]$; (*b*) $[N(PPh_3)_2][B]$ + impurity of $[N(PPh_3)_2][A]$; A and B as in Fig. 4

most probable primary reduction product, the trimercury cluster trianion $[Os_{18}Hg_3C_2(CO)_{42}]^{3-}$, is not observed in the chemical or electrochemical reduction it must be a very short-lived species which rapidly extrudes mercury to give either the dimercury trianion **4** or the disproportionation products **1** and **3**, the latter process partially regenerating the starting material. Both possibilities are compatible with the data presented here.

Conclusion

The aim of this study was the investigation of the reactivity of $[N(PPh_3)_2]_2[Os_{18}Hg_3C_2(CO)_{42}]$ **1**, a high-nuclearity Os–Hg cluster with a 'built-in' site of metal-core reactivity, first towards chemical reducing agents and secondly under the conditions of electrochemical reduction. The mercury-extrusion product, $[N(PPh_3)_2]_4[Os_{18}Hg_2C_2(CO)_{42}]$ **3**, was structurally characterised by X-ray crystallography and shown to have a structure related to that of its dianionic analogue, $[N(PPh_3)_2]_2[Os_{18}Hg_2C_2(CO)_{42}]$ **2**, reported previously as the product of photolytic extrusion of Hg from **1**; this pair is thus a rare example of a cluster structurally characterised in two oxidation states.

Along with the photochemical studies of compound **1** this work provides support for the concept of tuned reactivity by local metal–metal bond labilisation in extended cluster-core structures. Further investigations along these lines are currently underway.

Experimental

All manipulations were performed under an inert-gas atmosphere of dried argon or nitrogen in standard (Schlenk) glassware. Schlenk tubes and other reaction vessels were evacuated and flamed with a bunsen burner prior to use. Solvents and solutions were transferred from one reaction vessel to another with the aid of stainless-steel canulae under complete exclusion of air and moisture ('canula/septa technique'). Solvents were dried according to standard procedures and saturated with Ar or N_2 before use. The compound $[N(PPh_3)_2]_2[Os_{18}Hg_3C_2(CO)_{42}]$ was prepared as described in ref. 4. All other reagents were obtained commercially and used as purchased without further purification. The ^{13}C-enriched samples used for the ^{13}C NMR studies reported in this work were synthesised from ^{13}C-enriched $[Os_3(CO)_{12}]$.[9]

Solution infrared spectra were recorded in NaCl or CaF_2 cells (path length 0.5 mm) on a Perkin Elmer or 1710 Fourier-transform spectrometer. Fast atom bombardment (FAB) mass spectra were obtained on a Kratos MS50 spectrometer. The matrix used was either 3-nitrobenzyl alcohol or thioglycerol and the calibrant CsI. The isotope distributions of parent ions were simulated with a computer program implemented on the DS90 data system of a Kratos MS890 mass spectrometer. The ^{13}C NMR spectra were recorded on a Bruker AM 400 Fourier-transform spectrometer. Deuteriated solvents were used in all experiments, and the resonance of the residual protons or the natural-abundance ^{13}C were used as internal secondary chemical shift reference (*vs.* tetramethylsilane).

The electrochemical experiments were performed using an AMEL model 553 potentiostat with a standard three-electrode set-up. Cyclic voltammograms were obtained using a platinum-bead working electrode and a similar auxiliary electrode; the reference electrode in all experiments was a Ag–AgCl (aq) electrode. The effects of solution resistance were minimised by working with highly dilute (10^{-5}–10^{-4} mol dm^{-3}) solutions of the sample and small electrodes, so that peak currents were generally low. All potentials are cited against Ag–AgCl and are uncompensated for resistance effects of liquid-junction potentials which are assumed to be constant throughout the experiment. Using this reference, the $E_{\frac{1}{2}}$ value for ferrocenium–ferrocene was +540 mV in CH_2Cl_2 in good agreement with literature values.[10] Scan rates were between 20 and 400 mV s^{-1} with 100 mV s^{-1} as the standard rate. The supporting electrolyte was tetra-*n*-butylammonium tetrafluoroborate (*ca.* 0.05 mol dm^3). Solutions in the electrochemical cell were purged with N_2 for *ca.* 15 min prior to the recording of a cyclic voltammogram and were maintained under N_2 throughout the experiment.

$[N(PPh_3)_2]_4[Os_{18}Hg_2C_2(CO)_{42}]$ **3**.—(*a*) The compound $[N(PPh_3)_2]_2[Os_{18}Hg_3C_2(CO)_{42}]$ **1** (50 mg, 7.9×10^{-7} mol) was dissolved in thf (20 cm^3). On addition of a solution (1 cm^3) of $[Co(\eta^5\text{-}C_5H_5)_2]$ (9×10^{-6} mol dm^{-3}) a slight change in colour from purple to a less-intense violet occurred immediately. The salt $[N(PPh_3)_2]Cl$ (40 mg) was added and the mixture stirred for 10 min. The solvent was then removed and the residue taken up in acetone (*ca.* 5 cm^3). The $[N(PPh_3)_2]^+$ salt of the tetraanionic cluster could be precipitated by careful addition of diethyl ether (2–3 cm^3) to yield 52 mg (92%) of **3** as a black microcrystalline material. Crystals suitable for X-ray crystallography were obtained by slow vapour diffusion of diethyl ether into the acetone solution. IR (acetone): ν(CO) 2047m, 2029s, and 1980s cm^{-1}. ^{13}C NMR [100.6 MHz, 50% ^{13}C-enriched sample, in $(CD_3)_2CO$ at 295 K]: δ 390.1 (interstitial carbide), 190.1 (6 CO), 187.1 [12 CO, $^2J(^{199}Hg\text{–}^{13}C)$ = 42 Hz], 186.3 (6 CO) and 178.9 (18 CO). Most abundant isotopomer of the molecular ion in the negative-ion FAB mass spectrum: dianion, *m/z* 2513 (simulated 2515); monoanion, *m/z* 5028 (simulated 5029).

(*b*) Compound **2** (30 mg, 4.9×10^{-6} mol) was dissolved in thf (20 cm^3). This solution was carefully titrated with a solution of

sodium–benzophenone (*ca.* 20 mg Na, 160 mg Ph_2CO in 15 cm^3 thf). The reduction was monitored by IR spectroscopy which showed the initial generation of the trianionic cluster $[Os_{18}Hg_3C_2(CO)_{42}]^{3-}$ **4** [ν(CO) (thf): 2051s, 2044vs and 1993s cm^{-1}] and, subsequently, the clean conversion into the tetraanion. After addition of $[N(PPh_3)_2]Cl$ (20 mg) the product was worked up as described above. Yields obtained were in the range of 85–90% based on **2**. The spectroscopic data for the product were identical to those cited above.

$[N(PPh_3)_2]_3[Os_{18}Hg_2C_2(CO)_{42}]$ **4**.—A solution of $[N(PPh_3)_2]_2[Os_{18}Hg_2C_2(CO)_{42}]$ **2** (20 mg, 3.3×10^{-7} mol in 10 cm^3 thf) was carefully titrated into a solution of $[N(PPh_3)_2]_4[Os_{18}Hg_2C_2(CO)_{42}]$ **3** (20 mg, 2.8×10^{-6} mol in 10 cm^3 thf). The comproportionation reaction was monitored by IR spectroscopy and **2** added until the conversion into **4** was complete (*ca.* 8.5 cm^3 of the solution of **2**). The solvent volume was then reduced to *ca.* 5 cm^3 and the reaction product precipitated by addition of diethyl ether. IR (CH_2Cl_2): ν(CO) 2051s, 2044vs and 1994s cm^{-1}. Most abundant isotopomer of the molecular ion in the negative-ion FAB mass spectrum: dianion, *m/z* 2512 (simulated 2515); monoanion, *m/z* 5026 (simulated 5029).

Reaction of Compound **3** *with* Hg^{2+}.—Compound **3** (30 mg, 4.2×10^{-6} mol) was dissolved in thf (15 cm^3) and solid $Hg(O_3SCF_3)_2$ (2.2 mg, 4.4×10^{-6} mol) was added. The violet solution immediately turned deep purple and the generation of $[N(PPh_3)_2]_2[Os_{18}Hg_3C_2(CO)_{42}]$ **1** was confirmed by IR and mass spectroscopy. The reaction product was precipitated by addition of diethyl ether. Yield 25 mg (95% based on **3**).

Chemical Oxidation of Compound **3** *with* $[Fe(\eta^5\text{-}C_5H_5)_2]BF_4$.—A solution of $[N(PPh_3)_2]_4[Os_{18}Hg_2C_2(CO)_{42}]$ **3** (30 mg, 4.2×10^{-6} mol in 15 cm^3 thf) was titrated with a solution of $[Fe(\eta^5\text{-}C_5H_5)_2]BF_4$ (10 mg, 36.6×10^{-6} mol in 5 cm^3 thf). The redox reaction was monitored by infrared spectroscopy which initially indicated the formation of the trianionic cluster **4** and on further addition of the oxidant (overall *ca.* 1.2 cm^3) the generation of the dianion $[Os_{18}Hg_2C_2(CO)_{42}]^{2-}$ **2** which had identical spectroscopic properties (IR, mass) to those of the product otained photolytically from **1**.

X-Ray Crystallography of $[N(PPh_3)_2]_4[Os_{18}Hg_3C_2(CO)_{42}]$ **3**.— *Crystal data.* $C_{189}H_{122}Cl_2Hg_2N_4O_{42}Os_{18}P_8$, M = 7264.34, triclinic, space group $P\bar{1}$ (no. 2), a = 19.121(2), b = 16.638(4), c = 17.676(4) Å, α = 89.23(2), β = 117.24(2), γ = 94.03(2)°, U = 4986.23 $Å^3$, D_c = 2.419 g cm^{-3}, $F(000)$ = 3302. A dark crystal of size 0.30 × 0.18 × 0.12 mm, μ(Mo-Kα) = 130.9 cm^{-1}, was used in the data collection.

Data collection. Data were collected in the range θ 3–25°, with a scan width of 0.80°, using the technique described previously.[11] Equivalent reflections were merged to give 7222 data with $I/\sigma(I) > 3.0$. Absorption corrections were applied to the data after initial refinement with isotropic thermal parameters for all atoms.[12]

Structure solution and refinement.[13] The coordinates of the metal atoms defining the octahedron were deduced from a Patterson synthesis, and the remaining non-hydrogen atoms were located from subsequent Fourier difference syntheses. The phenyl rings were constrained to idealised hexagonal geometry (C–C 1.395 and C–H 1.08 Å) with fixed thermal parameters of 0.1 $Å^2$ assigned to the hydrogen atoms. Three residual maxima were interpreted as due to half a dichloromethane molecule in the asymmetric unit, and the parameters of these atoms of half occupancy refined satisfactorily. The osmium, mercury, phosphorus, chlorine and nitrogen atoms were assigned anisotropic thermal parameters in the final cycles of full-matrix refinement which converged at R 0.0609 and R' 0.0584 with weights of $w = 1/\sigma^2F_o$ assigned to the individual reflections.

Additional material available from the Cambridge Crystallographic Data Centre comprises H-atom coordinates, thermal parameters and remaining bond distances and angles.

Acknowledgements

We gratefully acknowledge the award of a Ph.D. scholarship by the Studienstiftung des deutschen Volkes (to L. H. G.) and financial support by ICI plc (to L. H. G.). We also thank the SERC for financial support and for access to the Chemical Database Service at Daresbury (M. McP.).

References

1 M. D. Vargas and J. N. Nicholls, *Adv. Inorg. Chem. Radiochem.*, 1986, **30**, 123.
2 L. H. Gade, B. F. G. Johnson, J. Lewis, M. McPartlin and H. R. Powell, (*a*) *J. Chem. Soc., Chem. Commun.*, 1990, 110; (*b*) *J. Chem. Soc., Dalton Trans.*, 1992, 921.
3 E. Charalambous, L. H. Gade, B. F. G. Johnson, T. Kotch, A. J. Lees, J. Lewis and M. McPartlin, *Angew. Chem., Int. Ed. Engl.*, 1990, **29**, 1137.
4 L. H. Gade, B. F. G. Johnson, J. Lewis, M. McPartlin, T. Kotch and A. J. Lees, *J. Am. Chem. Soc.*, 1991, **113**, 8698.
5 V. G. Albano, D. Braga, P. Chini, D. Strumolo and S. Martinengo, *J. Chem. Soc., Dalton Trans.*, 1983, 249; V. G. Albano, D. Braga, S. Martinengo, C. Seregni and D. Strumolo, *J. Organomet. Chem.*, 1983, **252**, C93.
6 J. Mason, *J. Am. Chem. Soc.*, 1991, **113**, 24.
7 P. Lemoine, *Coord. Chem.*, 1988, **83**, 169; W. E. Geiger, *Prog. Inorg. Chem.*, 1985, **33**, 275; S. R. Drake, *Polyhedron*, 1990, **9**, 455.
8 B. Tulyathan and W. E. Geiger, *J. Am. Chem. Soc.*, 1985, **107**, 5960; S. R. Drake, B. F. G. Johnson and J. Lewis, *J. Chem. Soc., Dalton Trans.*, 1987, 1051; M. H. Barley, S. R. Drake, B. F. G. Johnson and J. Lewis, *J. Chem. Soc., Chem. Commun.*, 1987, 1657.
9 L. R. Martin, F. W. B. Einstein and R. K. Pomeroy, *Organometallics*, 1988, **7**, 294.
10 C. LeVanda, K. Bechgaard, D. O. Cowan and M. D. Rausch, *J. Am. Chem. Soc.*, 1977, **99**, 2964.
11 M. K. Cooper, H. J. Goodwin, P. J. Guerney and M. McPartlin, *J. Chem. Soc., Dalton Trans.*, 1982, 757.
12 N. Walker and D. Stuart, *Acta Crystallogr., Sect. A*, 1983, **39**, 158.
13 G. M. Sheldrick, SHELX 76 program for crystal structure determination, University of Cambridge, 1976.

Received 27*th March* 1992; *Paper* 2/01628A